Earth and Planetary Science Letters 405 (2014) 52–61

Contents lists available at ScienceDirect

Earth and Planetary Science Letters

www.elsevier.com/locate/epsl

Explosive origin of silicic lava: Textural and δD–H_2O evidence for pyroclastic degassing during rhyolite effusion

Jonathan M. Castro [a,*,1], Ilya N. Bindeman [b], Hugh Tuffen [c], C. Ian Schipper [d]

[a] Institute for Geosciences, University of Mainz, Germany
[b] Department of Geological Sciences, University of Oregon, USA
[c] Lancaster Environment Centre, Lancaster University, UK
[d] School of Geography, Environment and Earth Sciences, Victoria University of Wellington, New Zealand

ARTICLE INFO

Article history:
Received 12 April 2014
Received in revised form 7 August 2014
Accepted 8 August 2014
Available online xxxx
Editor: B. Marty

Keywords:
obsidian
explosive lava
degassing
tuffisite
effusive
rhyolite

ABSTRACT

A long-standing challenge in volcanology is to explain why explosive eruptions of silicic magma give way to lava. A widely cited idea is that the explosive-to-effusive transition manifests a two-stage degassing history whereby lava is the product of non-explosive, open-system gas release following initial explosive, closed-system degassing. Direct observations of rhyolite eruptions indicate that effusive rhyolites are in fact highly explosive, as they erupt simultaneously with violent volcanic blasts and pyroclastic fountains for months from a common vent. This explosive and effusive overlap suggests that pyroclastic processes play a key role in rendering silicic magma sufficiently degassed to generate lava. Here we use precise H-isotope and magmatic H_2O measurements and textural evidence to demonstrate that effusion results from explosion(s)—lavas are the direct product of brittle deformation that fosters batched degassing into transient pyroclastic channels (tuffisites) that repetitively and explosively vent from effusing lava. Our measurements show, specifically that D/H ratios and H_2O contents of a broad suite of explosive and effusive samples from Chaitén volcano (hydrous bombs, Plinian pyroclasts, tuffisite veins, and lava) define a single and continuous degassing trend that links wet explosive pyroclasts ($\sim$ 1.6 wt.% H_2O, $\delta D = -76.4‰$) to dry obsidian lavas ($\sim$ 0.13 wt.% H_2O, $\delta D = -145.7‰$). This geochemical pattern is best fit with batched degassing model that comprises small repeated closed-system degassing steps followed by pulses of vapour extraction. This degassing mechanism is made possible by the action of tuffisite veins, which, by tapping already vesicular or brecciated magma, allow batches of exsolved gas to rapidly and explosively escape from relatively isolated closed-system domains and large tracts of conduit magma by giving them long-range connectivity. Even though tuffisite veins render magma degassed and capable of effusing, they are nonetheless the avenues of violent gas and particle transport and thus have the potential to drive explosions when they become blocked or welded shut. Thus the effusion of silicic lava, traditionally thought to be relatively benign process, presents a particularly hazardous form of explosive volcanism.

1. Introduction

Eruptions of silica-rich rhyolite magma are amongst the largest and most destructive on Earth. They exhibit the gamut of styles, and can progress from sudden and spectacular explosions (Melson and Saenz, 1973; Wilson, 1976; Hildreth and Fierstein, 2000; Castro and Dingwell, 2009; Alfano et al., 2011; Nguyen et al., 2014) and conclude in the emplacement of lava (e.g., Tuffen et al., 2013). Understanding what drives silicic magma through these eruptive extremes is one of the most important challenges in forecasting hazards during the course of a silicic eruption.

Disparate explosive and effusive eruption styles are believed to manifest the mechanisms of volatile separation that occur while the magma rises in the conduit. Most theoretical models, experimental, and field-based studies of rhyolite volcanoes link explosive and effusive styles to a two-stage degassing history that is controlled by time-varying magma ascent, conduit permeability, and deformation modes (Eichelberger et al., 1986; Jaupart and Allègre, 1991; Woods and Koyaguchi, 1994; Rust et al., 2004; Rust and Cashman, 2007; Adams et al., 2006). Explosive eruptions

* Corresponding author.
E-mail addresses: castroj@uni-mainz.de (J.M. Castro), bindeman@oregon.edu (I.N. Bindeman), h.tuffen@lancaster.ac.uk (H. Tuffen), schipper.ian@gmail.com (C. Ian Schipper).
[1] Tel.: +49 6131 392 4146.

http://dx.doi.org/10.1016/j.epsl.2014.08.012
0012-821X/

are considered to be driven by catastrophic release and expansion of gas from rapidly ascending bubbly magma (Sparks, 1978) that inevitably fragments by a number of different mechanisms (Alidibirov and Dingwell, 1996; Dingwell, 1996; Papale, 1999). In this regime, bubbly magma behaves as a chemically closed system (Taylor et al., 1983; Newman et al., 1988; Anderson and Fink, 1989; Villemant and Boudon, 1998; Cashman, 2004) in that exsolved volatiles remain in bubbles and in contact with the melt until the magma explosively fragments.

At the other end of the eruptive spectrum, effusive rhyolites are thought to record entirely different degassing and ascent dynamics than their explosive counterparts (Eichelberger et al., 1986; Cabrera et al., 2011; Okumura et al., 2009). The products of effusion, characteristically thick ($>$ 40 m) masses of glassy lava (Figs. 1, 2), are sourced from the same hydrous magma that fuels Plinian eruptions (Castro et al., 2013), yet are largely devoid of their original magmatic H_2O (Eichelberger and Westrich, 1981; Newman et al., 1988; Castro and Mercer, 2004). Thus, lava's degassed nature and dense and coherent form suggests paradoxically, that magma fuelling lava eruptions outgasses more efficiently than magma that produces pyroclasts. To explain "non-explosive silicic volcanism", Taylor et al. (1983) and Eichelberger et al. (1986) proposed that silicic lavas were once chemically open systems that degassed quiescently as highly permeable magmatic foams that later collapsed upon extrusion. According to this model, the transition from explosive to non-explosive volcanism reflects changes in the rates of shallow magma supply and ascent, which need to decrease, and vent permeability, which must increase (Jaupart and Allègre, 1991; Woods and Koyaguchi, 1994). In this way, open-system degassing is achieved while the magma is still in a coherent yet bubbly state and the efficiency of degassing through frothy magma prevents fragmentation. More recent studies of rhyolite volcanoes offer variations on this theme, but suggest that open-system degassing conditions may also be achieved by non-explosive, shear-induced brittle deformation of magma at or near the conduit margins (Gonnermann and Manga, 2003; Rust et al., 2004; Cabrera et al., 2011; Okumura et al., 2009, 2010); such brecciation would provide sites for diffusive particle degassing and avenues for exsolved fluids to leak out and dissipate gas overpressure that would otherwise drive explosivity. Castro et al. (2012) assessed the feasibility of melt-fracture degassing by measuring H_2O concentration-gradients around the margins of fracture-bounded pyroclastic veins in order to measure the amount of local gas loss in bombs produced in the first scientifically observed rhyolite eruption (volcán Chaitén, Chile, May, 2008). They determined that diffusive degassing of fractured magma along the conduit margins is not a time-effective mechanism to bleed off excess volatile pressure and make lava, unless the fractures are numerous and tapping already vesicular magma whose bubbly state would foster permeable outgassing. Most recently, experimental evidence (Okumura et al., 2013) indicates that shear localization in bubbly rhyolite may actually suppress outgassing at the conduit margins, and instead could promote sustained explosive eruptions.

Recent eruptions at Chaitén and Cordón Caulle volcanoes (Chile) have provided unprecedented opportunities to directly observe the course and sample the products of rhyolite eruptions and thus, test theories linking explosive and effusive volcanism to contrasting patterns of magma degassing and ascent (Castro and Dingwell, 2009; Castro et al., 2012, 2013, Schipper et al., 2013). In this paper we address the question: do explosive and effusive eruption styles (exhibited by rhyolite magma) reflect fundamentally different degassing mechanisms? The striking observation during these eruptions, which will be chronicled in detail in the next section, is that effusive eruptions *are* explosive—lava erupts from the same vent as, and simultaneously with, vigorous pyroclastic fountains (Fig. 1; Supplementary Video), large bomb-generating blasts, and persistent ash jets during most of the effusive phase (Schipper et al., 2013). This pattern of hybrid and juxtaposed volcanic activity is wholly inconsistent with existing two-stage degassing models because these models treat explosive and effusive eruptions separately (Eichelberger et al., 1986; Newman et al., 1988; Gonnermann and Manga, 2003; Rust et al., 2004). The hybrid activity at Chaitén and Cordón Caulle instead suggests that lava and pyroclasts are intrinsically linked by a common degassing mechanism. In this paper we present textural and geochemical evidence that demonstrates that the dominant mechanism of gas loss during effusive activity is pyroclastic activity involving shattered magma that moves as fragment-laden currents through transient channels (tuffisites; Heiken et al., 1988) within the magma-filled conduit. We have measured the H_2O and H-isotopic compositions of intermixed pyroclastic and effusive rhyolites to demonstrate a unique degassing path that links pyroclasts to lava, and therefore explosive and effusive volcanism.

2. Volcanological context

2.1. Simultaneous explosive and effusive venting at Chaitén and Cordón Caulle, Chile

Rhyolite eruptions at Chaitén (2008) and Cordón Caulle (CC; 2011) followed nearly identical patterns beginning with Plinian eruptions (Lara, 2009; Castro and Dingwell, 2009; Castro et al., 2013; Major and Lara, 2013) that within days graded into pyroclastic flows and fountains of fluctuating height (3–10 km). Fountaining coincided with frequent (10s per hour) explosions that cast metre-sized blocks to kilometres from the vents. Lavas effused on the tenth day of each eruption while pyroclastic fountains and explosions continued from the same vents (Fig. 1). After several weeks, the pyroclastic activity became organized within the lavas' points of emergence into several discrete "sub-vents" (Schipper et al., 2013), each of which displayed cycles of ash jetting and bomb blasts (Supplementary Video). Lava effusion and concurrent ash and bomb explosions continued for several months at both volcanoes, until after more than a year of hybrid activity, pure lava effusion (at CC) and spine-growth (at Chaitén) closed the final stages of eruption (Lara, 2009; Castro et al., 2013; Tuffen et al., 2013; Major and Lara, 2013).

2.2. Tuffisites: pyroclastic pathways through emergent lava

As demonstrated by Schipper et al. (2013), the ash-to-blast eruption cycles that persistently accompany lava effusion (Supplementary Video) likely manifested the deep-seated transport of pyroclasts and gas through channels that transected lava-forming magma and extended to considerable depth (10's to 100's of m) in the conduit. These pyroclastic channels are now preserved in varying amounts (10–50 vol.%) within both lavas and bombs as variably welded fragment-filled veins and tubular channels, termed "tuffisites" (Heiken et al., 1988; Stasiuk et al., 1996; Tuffen et al., 2003; Tuffen and Dingwell, 2005; Castro et al., 2012). Tuffisites are found in bombs that were erupted in the opening days of activity at both Chaitén (Castro et al., 2012) and Cordón Caulle (Schipper et al., 2013), and in the lavas that began to erupt in the second week (Fig. 2), indicating that they are ubiquitous features that record persistent degassing processes across several months of explosive and effusive activity. Tuffisites are also ubiquitous in the conduits of several other rhyolite volcanoes (Heiken et al., 1988; Stasiuk et al., 1996; Tuffen and Dingwell, 2005), and these observations collectively reinforce the notion that tuffisites are pervasive in both space and time.

Fig. 1. Synchronous explosive and effusive rhyolite eruptions at (a) Chaitén, and (b, c) Cordón Caulle volcanoes, Chile. The photo in (a) shows hybrid explosive–effusive activity on 28 May, 2008 (photo by Jeffrey Marso, USGS), about two weeks after obsidian lava (reddish flow LHS) began effusing from the explosively erupting vent. The lava in this picture is about 300 m in long dimension. A nearly identical progression towards hybrid activity was observed at Cordón Caulle (b), and produced a voluminous obsidian lava flow (black in foreground and grey landscape in background) and continued for about 10 months from the onset of obsidian effusion (photo by Alejandro Sotomayer on 14 February 2012). (c) Explosive–effusive activity at Cordón Caulle produced obsidian lava, evident as dark arcuate lobes at centre and bottom of photo (Alejandro Sotomayer on 14 February 2012), and abundant ash and coarse (~ metre scale) bombs (arrows) for nearly a year.

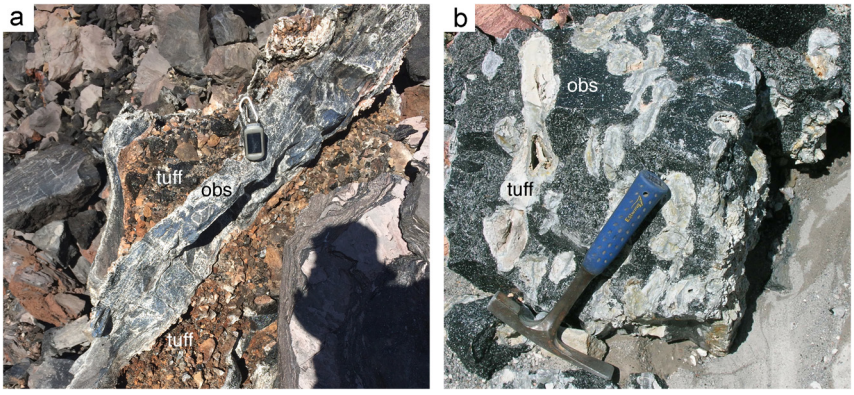

Fig. 2. Tuffisitic lava comprising pyroclastic channels (tuff) set in dense glassy rhyolite at Cordón Caulle (a) and Chaitén (b; photo courtesy of Jake Lowenstern). These exposures of tuffisite rest at the flow perimeters and are therefore representative of pyroclastic degassing of lava during earliest stage of effusion, when accompanying explosive activity was most vigorous. The pyroclasts in the Cordón Caulle lava are coarse and mostly unconsolidated, whereas those in Chaitén are denser, and form discontinuous bands (cm's thick) that have been deformed into boudinage structures during flow advance.

Tuffisites range widely in size (mm's – m's) and comprise diverse mixtures of vitric ash (grain size ~ μm to mm), pumice, and obsidian fragments (~ mm to cm). In obsidian lavas, tuffisites are found over a remarkably broad range of scales, occurring as large (m's) domains of variably welded and deformed pyroclastic materials that fill channel-like structures near flow fronts (Fig. 2), and as thin (cm's–mm's), yet highly elongate flow bands that contain relict porosity and remnant glass shard structures (Figs. 3, 4). Tuffisite veins in ballistic bombs crosscut both dense glassy and highly vesicular patches, and are linked by fracture networks that themselves contain minor inclusions of pumice, obsidian fragments and vesicle chains. These fractures must have been much more open than they are at present in order to convey particles many times larger than their current crack widths (Fig. 4). That the fractures still contain some particles suggest that they probably acted like tuffisites but more efficiently discharged their pyroclasts before closing.

As tuffisites are the variably welded remnants of pyroclastic fountains that once vented from emerging lava, they must hold valuable clues as to how rhyolite degasses (e.g., Castro et al., 2012; Berlo et al., 2013). Their abundance in both explosive (bombs) and effusive (obsidian lava) materials, along with visual records of repeated gas-and-ash jetting and bomb explosions during effusion (Castro et al., 2013; Schipper et al., 2013) suggests that tuffisites play a central role in sustaining long-lived pyroclastic activity while at the same time promoting voluminous effusion of degassed lava. In order to evaluate how tuffisites mediate between explosive and effusively erupted rhyolite magma, we have measured the bulk H_2O and hydrogen isotopic compositions of tuffisites and co-eruptive rhyolites from Chaitén and Cordón Caulle volcanoes.

3. Samples and analytical methods

We measured bulk magmatic H_2O and its H-isotopic composition of lavas, tuffisitic veins, pumiceous pyroclasts, and vein-hosting obsidians in order to track the chemical evolution of melt and coexisting hydrous fluid phase during magma degassing across explosive, hybrid, and effusive stages of activity at Chaitén and Cordón Caulle volcanoes, Chile (e.g., Taylor et al., 1983; Newman et al., 1988; Anderson and Fink, 1989; Villemant and Boudon, 1998). Samples for hydrogen isotopic and bulk H_2O analyses were collected from the 2008–2010 eruptive units at Chaitén and 2011 units at Cordón Caulle. Our strategy was to assemble a suite of the explosive and effusive products that represent the full eruption spectrum. This meant that, in addition to Plinian pumice fall deposits and obsidian lava, we collected samples of glassy and pumiceous tuffisite-hosting bombs (Fig. 4) that represent the pyroclastic activity continuing from the Plinian phase and overlapping with effusive activity. Bombs were collected over areas of approximately 4 km^2 adjacent to the lava flows at Chaitén and Cordón

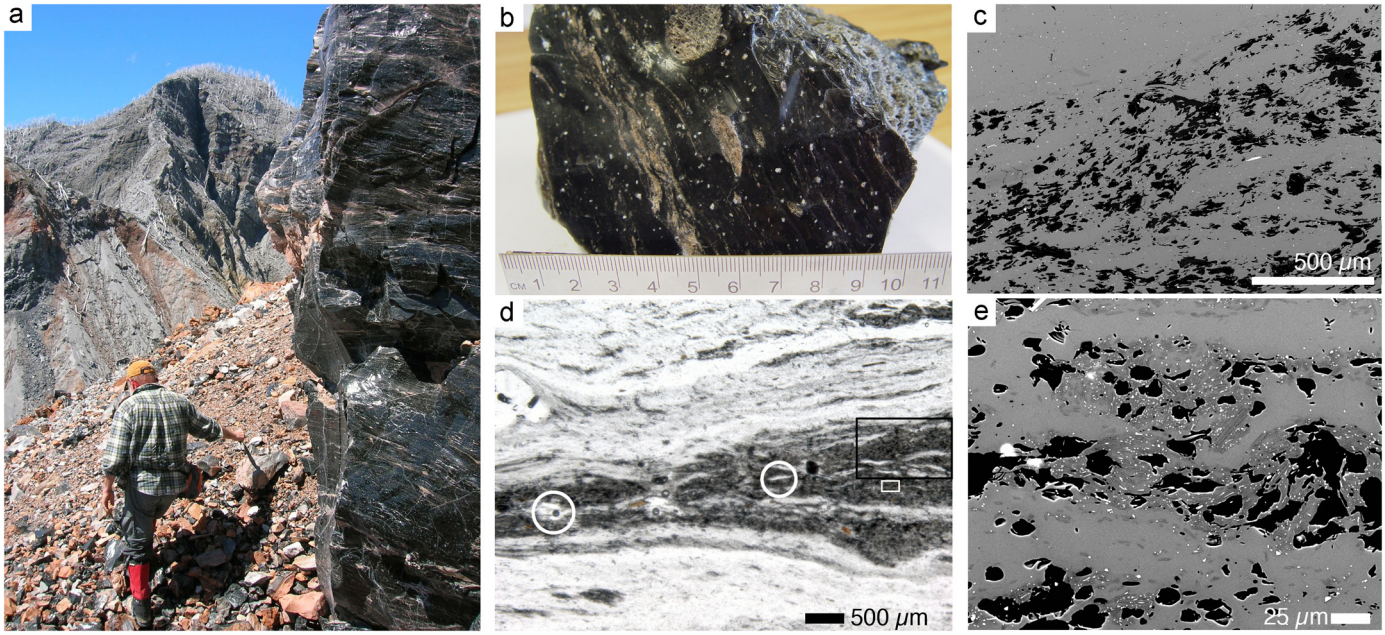

Fig. 3. Rhyolitic obsidian lava erupted in May 2008 at Chaitén volcano, Chile. This outcrop (a) and others like it served as the source for some lava samples (e.g., MT4; JC1A) measured in this study. In (a) John Eichelberger stands by the black, flow-banded obsidian flow front. Obsidian samples contain abundant tuffisitic layers (reddish seams in a), which have been deformed considerably during their eruption (b). The tuffisite bands retain considerable porosity (~ 30 vol.% voids) despite being flattened (c). The back-scattered electron image in (c) is a magnified view of the area shown in the black box in photomicrograph in frame (d). Individual glass shards (d; encircled) can be discerned from the surrounding sintered, microclastic matrix (e). The photomicrograph shown in (e) is a magnified view of the small white box in frame (d) and illustrates the fragile, high porosity channels that once served to deliver gas from the rising magma. Many of the pores are lined by microlite-rich glass (dominantly feldspar and Fe-oxide), which may reflect the influence of H_2O fluid and trace element transport through the veins (Berlo et al., 2013).

Caulle. The exact eruption timing of the bombs is unknown, but evidence for their recent deposition, which includes the observation that they rest on top of or made craters that penetrated into the Plinian fall deposits, provides firm evidence that they began to erupt after the first two to three days of activity (SERNAGEOMIN activity reports). Plinian pyroclasts (both pumiceous and dense obsidian) were sampled as discrete lapilli from fall deposits (Castro and Dingwell, 2009; Castro et al., 2012, 2013). Bombs and lavas comprise large (10s of cms) glassy and pumiceous blocks on the crater rim, lava flow fronts, and flanks of each volcano. The bombs were photographed and then cracked open in order to sub-sample material from their interiors.

All tuffisite veins and glassy host samples were drilled out of the interior of the bombs and lava blocks with a 1 cm diameter diamond coring drill. Analyses were made on obsidian–tuffisite pairs comprising samples positioned adjacent to one another within a bomb sample (Fig. 4a). These aliquots were then immediately dried in a vacuum oven for 24 hrs at 100 °C in order to drive off any absorbed water from the drill. Afterwards, the samples were crushed and sieved to between 125 and 200 μm size. The location of the samples from well within the interior of the bombs and lavas means that they were chemically untouched by surface waters.

Thermal Conversion Element Analyzer (TCEA) mass spectrometry measurements, used to detect bulk H_2O and H-isotopic composition (Bindeman et al., 2012; Nolan and Bindeman, 2013), were performed at the University of Oregon and made in triplicate on rhyolite powders ranging in mass from 4–12 micrograms. Weighing was performed on an analytical balance with 6-digit precision. Powders were then loaded into silver foil capsules and folded shut. The analyses, performed following the techniques of Nolan and Bindeman (2013), on a TCEA-MAT 253 system, yield δD_{smow} ($= [(^2H/^1H)_{sample}/(^2H/^1H)] - 1\} \times 10^3$ where SMOW is standard mean ocean water) values to within ±3‰ and H_2O to ±0.01 wt.%. The reproducibility of δD_{smow} is excellent and uncertainty of bulk water measurements is estimated to about 10% as assessed by independent spot H_2O measurements made on the same samples by synchrotron micro-FTIR (Castro et al., 2012).

Tuffisite vein and adjacent bomb- and lava-host major element compositions were measured in order to confirm that tuffisite and hosting rhyolite represent members of the same magmatic suite. Measurements were performed on ground bulk powders extracted from veins and adjacent bomb-host material using a Phillips XRF instrument (MagiXPRO-XRF). Analyses were made in duplicate and carry an analytical precision of 10% relative.

4. Analytical results

Chaitén and Cordón Caulle eruption products maintain constant major element compositions irrespective of eruption mode and sequence (Supplementary Table S1). This indicates that tuffisitic veins are derived from the same magma that produced the bombs and lavas.

4.1. Cordón Caulle bulk H_2O and D–H relations

H_2O contents are uniformly low (< 0.35 wt.%; Fig. 5; Supplementary Information) in the Cordón Caulle eruption products (Schipper et al., 2013), and no systematic differences in either δD or H_2O exist for the various eruptive phases and products (Fig. 5). Early-erupted (4 June 2011) Plinian pumice, for example, is as degassed as later erupted glassy and pumice breccia bombs, but two Plinian clasts exhibit the highest δD of the suite at very low H_2O contents between ~ 0.1 and 0.2 wt.%. One tuffisite–obsidian pair (CC pair 1; Table 1) exhibits a change in both H_2O and δD across the tuffisite obsidian border, whereby the host obsidian is more hydrous and enriched in deuterium compared to the tuffisite vein. Patterns like this one are also observed in the Chaitén samples (Section 4.2). There is a general decrease in the δD with falling bulk H_2O, the values of which reach a minimum of about −135‰ at about 0.05 wt.% H_2O. Despite this decline in δD with falling H_2O, a well-defined degassing trend spanning several tens of ppm δD

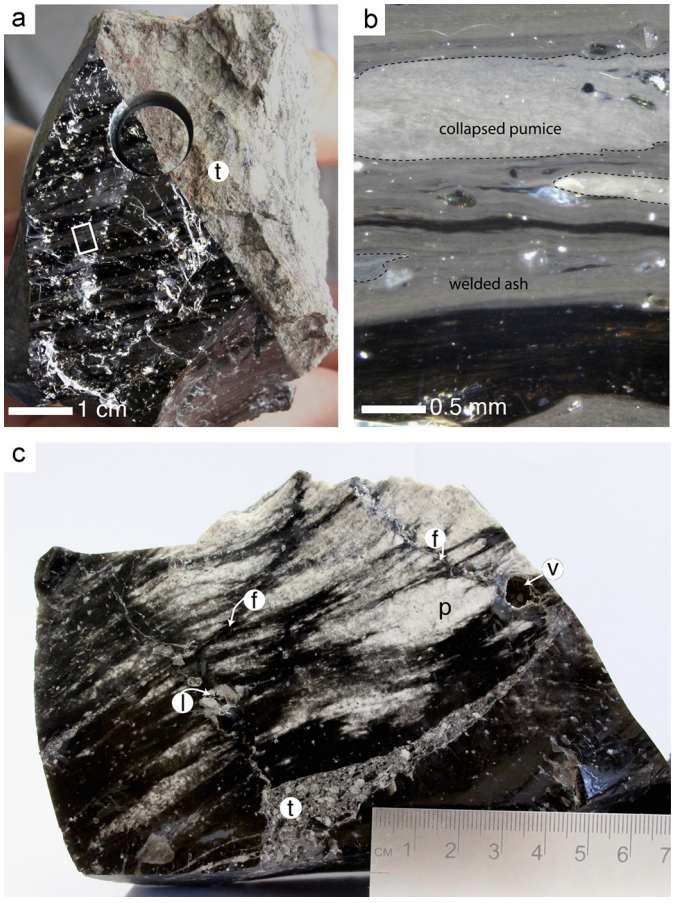

Fig. 4. Volcanic bombs produced at Cordón Caulle (a, b) and Chaitén (c) highlighting important textural and structural traits related to degassing. In (a) obsidian (black, left) is juxtaposed against a tuffisite vein (t) comprising pumice lapilli and ash (reddish). The circular drill core shows how adjacent obsidian–tuffisite pairs were subsampled from bombs. The flow bands in the dense obsidian form alternating stripes of un-disrupted black glass and light grey obsidian (white box) with clearly pyroclastic textures, evident in the magnified photomicrograph at right (b). These bands derived from formerly active tuffisite veins that later collapsed and annealed, indicating a repeated fracture-healing process (Tuffen et al., 2003). In the Chaitén bomb (c), several generations of tuffisite veins are evident, including one comprising brecciated pumice and obsidian lapilli set in a fine sintered ashy matrix (t). This vein cross-links two earlier and nearly completely sealed tuffisite veins, (f), which cut across vesicular zones (p) and still contain relict pumice clasts (l) that did not escape or completely densify. These sealed tuffisites are also lined with chains of large vesicles (v) that in turn contain clasts of pumice and obsidian, again reflecting the closure of a tuffisite vein followed by reorganization of the gas that remained between the particles.

and tenths of wt.% H_2O, as exemplified by Chaitén (next section) and many other explosive–effusive rhyolite sequences (Taylor et al., 1983; Newman et al., 1988), is lacking. This likely reflects the dry character of the Cordón Caulle magma, which could have contained as little as 2.5 wt.% pre-eruptive H_2O (Castro et al., 2013), a likely consequence of very shallow and hot magma storage ($\sim 900\,^{\circ}C$; Castro et al., 2013). Indeed, compared to other rhyolites (e.g., Newman et al., 1988; Castro et al., 2012; Castro and Mercer, 2004), the Cordón Caulle magma would have had lower melt viscosity stemming from its lower bulk SiO_2 (~ 70 wt.%; Supplementary Information) and higher eruptive temperature, factors of which would both promote higher diffusive degassing rates compared to higher-Si rhyolites (e.g., Chaitén; Castro and Dingwell, 2009; Castro et al., 2012).

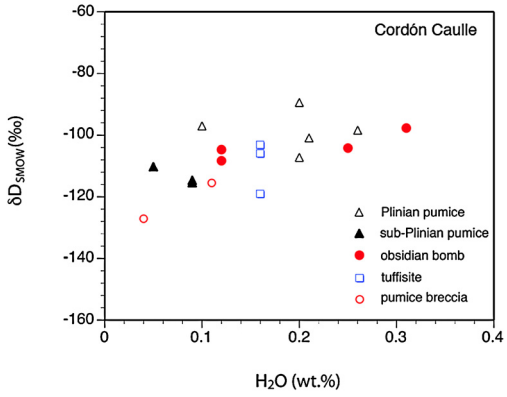

Fig. 5. δD and bulk-H_2O compositions of Cordón Caulle 2011–12 eruption products. Plinian pumice (erupted June 4, 2011) and later erupted pumice and obsidian bombs (erupted January 2012) have overlapping compositions and thus no degassing path can be deduced from this data. Tuffisite samples are obsidian bomb hosted (one with $\delta D \sim -120‰$), or are found cutting through pumice blocks (two with higher δD's ~ -105 to $-110‰$). The lack of a broad range in H_2O as observed at other rhyolite volcanoes precludes analysis of degassing signatures in the chronology of eruptive units.

4.2. Chaitén bulk H_2O and D–H relations

The Chaitén eruptives exhibit considerably more variation in bulk H_2O (~ 1.6–0.1 wt.%) and δD (~ -76 to $-145‰$) compared to Cordón Caulle. The Chaitén products can be grouped into two categories (Fig. 6a): 1) tuffisites and Plinian pumice pyroclasts with relatively high δD ($> -105‰$) and intermediate to low H_2O (~ 0.4–1.0 wt.%), and 2) dense obsidian and pumice bombs and lava, spanning a broad range of δD (~ -75 to $-150‰$) and H_2O (~ 0.1 to 1.6 wt.%). Two outliers are an obsidian clast from the Plinian deposit that plots within bomb-lava group, and an H_2O-rich tuffisite, also plotting on that trend (Fig. 6a).

Aside from one obsidian–tuffisite couple with identical H_2O and δD (pair 8; Fig. 6a), the Chaitén obsidian–tuffisite pairs exhibit remarkable compositional heterogeneity across very small ($\sim$ cm) length scales (Table 1). Tuffisites are drier than the hosting obsidians in all but two cases (pairs 4 and 10), and show variable δD depletion and enrichment with respect to their hosts. Tuffisites with lower δD than their host also have lower bulk H_2O (pairs 1, 2, 3, 5). By contrast, two tuffisites with higher δD are more hydrous than their hosts (pairs 4, 10). Finally, three tuffisites (pairs 6, 7, 9) are δD-enriched, despite being drier than the obsidian hosts.

5. Discussion

5.1. Modelling isotopic partitioning during degassing: closed, open, and batched cases

The δD–H_2O relations in co-eruptive obsidians and tuffisites reflect isotopic partitioning driven by degassing of hydrous fluid (e.g., Taylor et al., 1983) and can be modelled to test degassing mechanisms that prevail during pyroclastic and effusive activity. Because deuterium (D) is preferentially partitioned into the vapour phase (Taylor et al., 1983), subtle to extreme D/H fractionation will occur in response to progressive closed- and open-system degassing, respectively (Taylor et al., 1983). These two end-member degassing scenarios, acting in sequence, comprise the two-stage degassing path that is often cited to explain the explosive-to-effusive transition (e.g., Newman et al., 1988; Dobson et al., 1989; Rust et al., 2004; Adams et al., 2006).

In a closed system, the melt and exsolved fluid remain in contact and equilibrate throughout their association. These conditions may hold in a bubbly magma that has not reached a critical vesicularity to promote effective melt-gas separation via permeability

Table 1
Bulk H_2O and H-isotopic compositions of rhyolites from Chaitén and Cordón Caulle volcanoes.

Sample	Eruption unit	H_2O (wt.%)	δD_{smow} (‰)	Pair keyed to Fig. 6
Chaitén (2008)				
Ch-5a	pumiceous-Plinian	0.72	−90.3	
Ch-5b	pumiceous-Plinian	0.69	−93.2	
Ch-5c	pumiceous-Plinian	0.79	−90.9	
Ch-5d	pumiceous-Plinian	0.68	−94.1	
Ch-5e	pumiceous-Plinian	0.73	−92.3	
CH1	obsidian pyroclast-Plinian	1.15	−92.5	
JC2A	pumiceous bomb	0.67	−100.5	
JC1A	lava, May 2008, obsidian	0.13	−145.7	
MT-4	lava, May 2008, obsidian	0.15	−140.6	
MT-5a	lava, May 2008, obsidian	0.2	−135.1	
Tuff-2	tuffisite-vein	0.44	−96.9	pair 7
Tuff-2	obsidian-bomb host	0.7	−103.8	pair 7
Tuff-3	tuffisite-vein	0.66	−93.4	pair 5
Tuff-3	obsidian-bomb host	1.17	−84.9	pair 5
Tuff-4	tuffisite-vein	1.2	−90.54	pair 4
Tuff-4	obsidian-bomb host	0.52	−107.8	pair 4
Tuff-5	tuffisite-vein	0.44	−97.1	pair 2
Tuff-5	obsidian-bomb host	1.49	−79.2	pair 2
Tuff-6	tuffisite-vein	0.56	−87.9	pair 3
Tuff-6	obsidian-bomb host	1.3	−84.7	pair 3
Tuff-7	tuffisite-vein	0.6	−99.5	pair 8
Tuff-7	obsidian-bomb host	0.6	−101.8	pair 8
Tuff-8	tuffisite-vein	0.87	−79.6	pair 1
Tuff-8	obsidian-bomb host	1.58	−76.4	pair 1
Tuff-9	tuffisite-vein	0.43	−97.4	pair 6
Tuff-9	obsidian-bomb host	0.9	−99	pair 6
Tuff-10	tuffisite-vein	0.42	−101.2	pair 9
Tuff-10	obsidian-bomb host	0.54	−111.2	pair 9
Tuff-11	tuffisite-vein	0.49	−98.3	pair 10
Tuff-11	obsidian-bomb host	0.21	−117.9	pair 10
Tuff-12	collapsed pumice bomb	0.22	−122.8	
Tuff-13	obsidian bomb	0.78	−95.2	
Tuff-15	pumice bomb	0.22	−126.5	
Cordón Caulle (2011)				
Puy-4-1m	pumiceous-Plinian	0.26	−98.4	
Puy-4-2m	pumiceous-Plinian	0.1	−97	
Puy-4-3m	pumiceous-Plinian	0.2	−89.4	
Puy-4-4m	pumiceous-Plinian	0.2	−107.2	
Puy-4-5m	pumiceous-Plinian	0.21	−100.9	
Puy-035	obsidian bomb breadcrusted	0.31	−97.7	
Puy-045	tuffisite-vein	0.16	−119.1	CC pair 1
Puy-045	obsidian-bomb host	0.25	−104.2	CC pair 1
Puy-049	pumice breccia bomb	0.16	−103.2	
Puy-049	pumice breccia bomb	0.16	−107.4	
Puy-060	obsidian-bomb host	0.16	−106	
Puy-061b	pumice breccia bomb	0.04	−127.1	
Puy-109a	pumice bomb core	0.03	−92.4	
Puy-109a	pumice bomb rim	0.11	−115.5	
Puy-115a	brown pumice lapilli sub-Plinian	0.1	−115.4	
Puy-115b	brown pumice lapilli sub-Plinian	0.05	−110.2	
Puy-115c	brown pumice lapilli sub-Plinian	0.1	−114.6	

(Eichelberger et al., 1986), or in a pyroclastic vein that has a relatively restricted lateral or vertical extent such that it cannot receive or transmit gas and particles over great distances. Under these conditions D/H fractionation is described by mass balance (Taylor et al., 1983):

$$\partial D_f = \partial D_i - (1 - F)10^3 \ln \alpha_{v-m}, \quad (1)$$

where ∂D_f is the final δD (in ‰) of the H_2O in the pyroclasts that have degassed in the crack, ∂D_i is the initial δD of the host melt and pyroclasts, F is the fraction of H_2O remaining in the host melt calculated as final H_2O (i.e., the value at the pressure drop) divided by the initial melt-H_2O (fixed and equal to the original magmatic value), and α_{v-m} is the hydrous-speciation dependant bulk H-isotope fractionation factor between hydrous vapour and rhyolite melt at 825 °C (Dobson et al., 1989). The isotopic shift in a perfectly closed system traces a linear trajectory and δD will diminish modestly (at most a few tens of ‰) for a relatively large decrease in bulk H_2O (e.g., several wt.%).

Degassing in an open system, by contrast, drives strong D/H fractionation, as there is immediate and continual removal of exsolved volatiles from the melt source, which prevents isotopic equilibrium between exsolved and dissolved H_2O in the melt. Because the amount of H_2O remaining in the melt continually drops, the isotopic fractionation can be quite large (several tens of ‰), as described by the Rayleigh distillation equation (Taylor, 1991):

$$\partial D_f = (\partial D_i + 1000)\left(F^{\alpha-1}\right) - 1000 \quad (2)$$

Here, all parameters are defined as before, except that ∂D_i is continually adjusted to lower values as volatiles are stripped away. Thus, the characteristically dry and strongly D-depleted signatures of obsidian flows have long been viewed as the hallmarks of open-system degassing during effusive rhyolite eruptions (e.g., Taylor et al., 1983; Eichelberger et al., 1986; Newman et al., 1988).

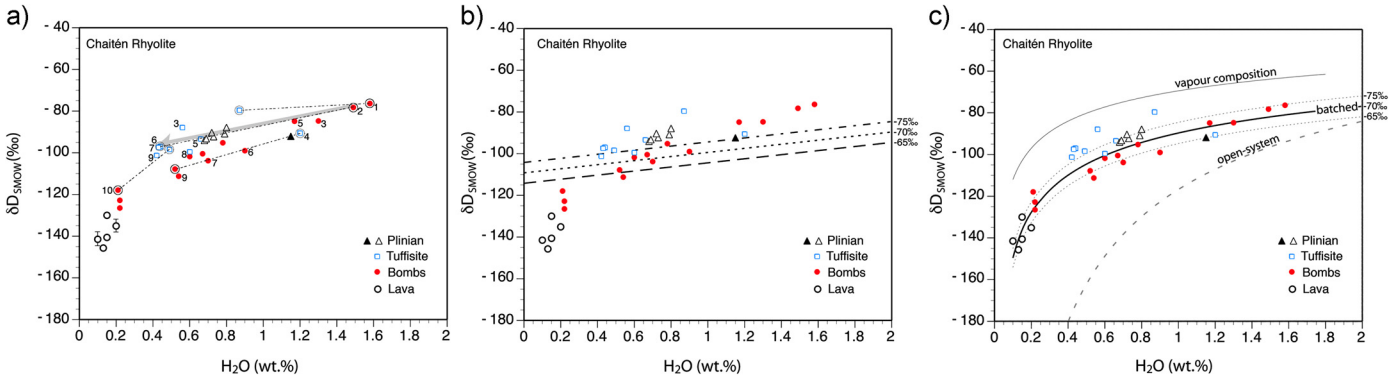

Fig. 6. δD–H_2O in Chaitén rhyolites erupted during the first fortnight of activity, beginning 1 May, 2008. Analytical variability of triplicate measurements (Nolan and Bindeman, 2013) is less than the symbol size ($< \pm 3$ ppm δD; and < 0.01 wt.% H_2O), or given with an error bar (in lava samples). (a) Plinian samples comprise pumice clasts (△) and one obsidian chip (▲). Bombs (●) contain fragmental tuffisite veins (□) and form a continuous trend in δD–H_2O space with the lavas (○). Dash-dotted lines and numbers on symbols link bomb-tuffisite pairs that were juxtaposed in the sample. Not all pairs have been indicated with tie lines for the sake of maintaining clarity. Pair numbers correspond to those given in Table 1. Tuffisites are more degassed, but may be δD-enriched or depleted relative to their bomb hosts. Of the isotopically lighter tuffisites, two are consistent with single-step closed-system degassing of their hosts (pairs 2 and 5). One such degassing path is shown as a bold grey arrow (for pair 2) and calculated with data from the ends of the arrow using Eq. (1), and an eruption temperature of 825 °C (Castro and Dingwell, 2009). Further model constraints are described in the text. (b, c) Chaitén δD-bulk H_2O data compared to, single-step closed (b) and (c) open-system and batched degassing models. The single-step closed-system model (dashed lines) shows three possible starting δD values (-75, -70 and -65‰) for degassing between 4.0 and 0.1 wt.% H_2O. In (c) the best-fit model is batched degassing (bold black curve; $R^2 = 0.865$), comprising repeated closed-system steps (0.1 wt.%; Taylor, 1991) and vapour removal after each step. The finely dashed curves are also batched degassing with different starting δD's indicated to the RHS. Coexisting vapour compositions produced during batched degassing are predicted via isotopic fractionation factors (Dobson et al., 1989). The bold grey dashed line gives an open-system degassing model result and highlights the inability of this style of degassing to generate compositions of highly degassed and D-depleted obsidian lavas.

A third style of degassing is the batch model or "multi-step open/closed" mechanism developed by Taylor (1991) to model the ca. 650–550 yr.b.p. eruptions of the Inyo Domes, CA rhyolite. This involves successive closed-system steps with intervening pulses of vapour extraction (i.e., batches). According to this model, a "quasi-open" state is achieved as batches of exsolved gas are periodically formed and removed during successive explosions. As the pulses of extracted batch gas gradually diminish bulk melt H_2O, δD undergoes a nonlinear decrease that steepens sharply at low total H_2O (i.e., the range of lava) due to the proportional rise in hydroxyl groups remaining in the melt (Dobson et al., 1989). Thus, even small batches of extracted H_2O will drive significant depletion of deuterium in the final stages of degassing. Batched degassing, therefore, encapsulates elements of both closed- and open-system behaviour with the important advantage that this mechanism can be linked to repetitive physical processes that control vapour exsolution, for example, ascent-driven decompression and rapid explosive gas release.

5.2. *Modelling degassing paths through Plinian pumice, tuffisites, bombs, and lavas*

Figs. 6b and 6c compare the δD–H_2O chemistry of Chaitén eruptives to closed-, open- and batched-degassing models. Recall that the Cordón Caulle data are too limited in bulk-H_2O to reveal a significant degassing trend, so here we focus solely on the Chaitén data. The bomb and lava compositions, which form a continuous trend that terminates in lava, are best fit by batched-degassing (Taylor, 1991) with initial melt-H_2O and deuterium content of 4 wt.% (Castro and Dingwell, 2009) and -70‰ respectively. Uncertainty in the position of the batched degassing path relates to the choice of the initial deuterium content, which is not known *a priori* but shifts the ensuing degassing path to higher or lower δD. We show two other model trends for initial δD of -65 and -75‰ to illustrate this shift and emphasize that this is the dominant source of uncertainty in the degassing path. In addition to the batched model fit, we also compare single-step closed (Fig. 6b) and open-system degassing (Fig. 6c) models to the data. Neither of these models captures the variation of the bomb, pumice pyroclast, and tuffisite compositions, and importantly, for a broad range of starting compositions and model conditions (Supplementary Information) both models fail to predict the compositions of obsidian lava at the end of the degassing trajectory, with closed-system greatly underestimating the depletion of δD and the open-system model overestimating δD depletion.

Although the batched degassing model fits the hydrous bombs and driest effusive rocks very well, there is still considerable variation of δD values in Plinian pumice, tuffisites and bombs on either side of this trend, especially in the range of ~ 0.4 to 0.9 wt.% H_2O. In this range, the bombs are more D-depleted than the model predicts, and tuffisites and Plinian pyroclasts generally more D-enriched. The bomb compositions could indicate that bomb-forming magma experienced some amount of open-system degassing in this composition interval. Indeed, since bombs are an amalgam of differently textured rhyolites (Fig. 4), including some that are highly vesicular and fractured rhyolite, the possibility exists that some domains were more chemically open on the mesoscale. Note however, that neither bombs nor lava have experienced the dramatic depletion in δD expected for pure open-system degassing as they plot well above the open-system degassing path (Fig. 6c; Supplementary Information). The bomb-lava trend therefore, likely reflects some D-buffering and possibly the thermo-mechanical reincorporation of tuffisitic veins, a D-rich source, into the magma to form flow-banded bombs and lava (Tuffen et al., 2003; Fig. 3).

Tuffisites and Plinian pyroclasts are δD-enriched (relative to the batched model), which could record the interaction of these pyroclastic materials with gasses derived from degassing of the bomb-forming magma. Note that the vapour exsolved during batched degassing is indeed isotopically heavier than the coexisting melt represented by the bomb compositions (cf. curve above and parallel to bomb path in Fig. 6c) and, together with the melt-degassing trend, brackets the tuffisitic and pumice pyroclastic compositions extremely well. This may explain the remarkable compositional similarity between the Plinian pumice and tuffisites and furthermore imply that tuffisitic degassing is the continuation of the high flux, gas-buffered conditions that fuel Plinian rhyolite eruptions (Newman et al., 1988; Rust et al., 2004).

In summary, the chemical patterns reflected in explosive and effusive products from Chaitén are consistent with a single batched

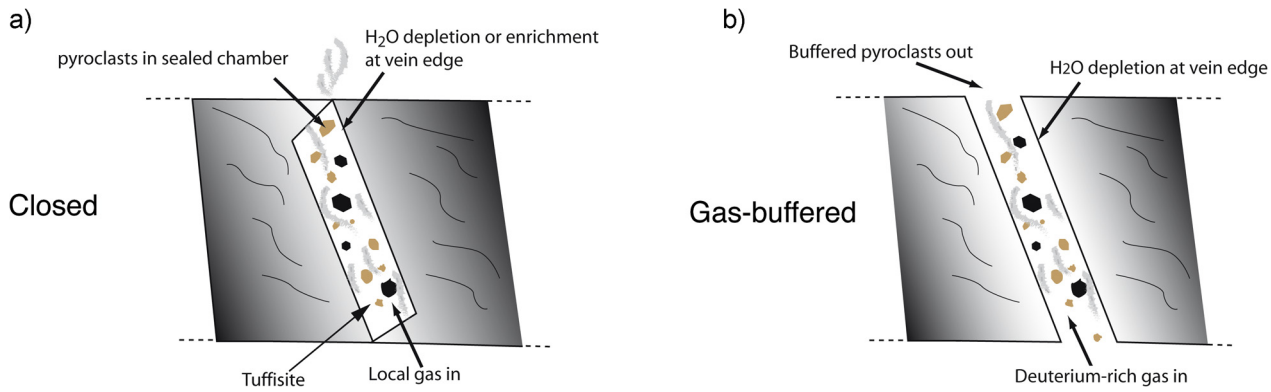

Fig. 7. Schematic diagrams showing two end-members of tuffisite behaviour inferred from cm-scale differences in δD and H_2O in bomb-host-vein couples. On the left, a closed-system degassing scenario arises from local melt fracturing and subsequent degassing into the crack. Pyroclasts may be derived locally and are degassed within the crack so that they equilibrate isotopically with the neighbouring melt. On the right, an open-buffered condition arises from tuffisite veins whose connectivity permits throughput of gas and particles. This may lead to gas buffering and enrichment of deuterium in degassing magma (Rust et al., 2004).

degassing mechanism involving repeated closed-system exsolution steps and ensuing pulses of vapour extraction. Complexity in the degassing path, manifested as compositional scatter of natural tuffisites and bombs about the model trend, may arise for a variety of reasons, including: 1) some degassing steps acted more openly, perhaps due to the physical state of magma (highly fractured and vesicular), 2) degassed vapour batches were larger than the modelled size (0.10 wt.%) resulting in less D-depletion per unit wt.% H_2O decrease, and/or 3) aliquots of batch gas were liberated and fluxed through other magma domains to buffer the D-contents of magma in different parts of the conduit. In the next section we examine in detail the cm-scale δD and H_2O variations between juxtaposed tuffisite and host-obsidian samples that support these interpretations and elucidate how pyroclastic veins actively collect and transmit gas, and therefore produce the degassing trend measured on the Chaitén eruptives (Fig. 6).

5.3. Eruptions at the vein scale: how tuffisites degas rhyolite magma

The Chaitén obsidian–tuffisite pairs exhibit remarkable variations in H_2O and δD over small length scales (cm). Most tuffisites are less hydrous than their hosts (Table 1), which is consistent with pyroclasts degassing within low-pressure cracks and veins (Cabrera et al., 2011; Castro et al., 2012; Fig. 6a). The pressure drops driving this degassing can be inferred from the H_2O content differences between host and tuffisite, assuming that these are equilibrium values dictated by pressure-dependent solubility (e.g., Newman and Lowenstern, 2002). Values determined in this way ($\sim$ 1–15 MPa) bracket a value ($\sim$ 3 MPa) determined by Castro et al. (2012) on similar tuffisitic bombs. Pressure drop estimates are *minima* because disequilibrium degassing would lead to greater volatile retention in the melt, and this would, in turn, mask what are effectively greater pressure drops.

Interestingly, two sample pairs (4 and 10; Table 1) comprise hydrous tuffisite embedded in drier obsidian, a configuration that could reflect the regassing of tuffisite due to pressurization of the vein after it had clogged and collapsed. The H_2O enrichments imply overpressures of $\sim$ 1 to 10 MPa, which are comparable to values inferred for the Mono Craters, rhyolite conduit (Watkins et al., 2012). Another explanation for the relatively hydrous tuffisites is that these pyroclasts were injected to shallower levels but did not have the time to degas and equilibrate to lower pressure before being explosively erupted and quenched in the bomb. Their higher water contents could therefore represent metastable values from greater depths (pressures) from which the ashes were derived. Viewed in this way, these hydrous tuffisites indicate relatively extensive down-conduit extension of the ash channels (Schipper et al., 2013), with some (pair 4; $\sim$ 1.2 wt.%) indicating upwards of 500 m vertical connectivity.

δD and H_2O relations across tuffisite-host borders reveal snapshots of degassing behaviour within pyroclastic veins. Two tuffisites have δD and H_2O consistent with closed-system degassing of the host melts (now glass) that encapsulate them (pairs 2 and 5). As shown in Fig. 6a, these tuffisite compositions can be predicted by closed-system mass balance (Eq. (1)) to within error of the measured isotopic values. This means that the magma host, vein-filling pyroclasts and exsolved vapour remained coupled until they were excavated (Fig. 7a), and were not fluxed by deeper-derived magmatic, or meteoric fluids (Rust et al., 2004; Supplementary Information). These tuffisites must have had limited spatial extents leading up to their explosive evacuation.

Most tuffisite–obsidian pairs, by contrast, record interaction with both local and distally derived magmatic fluids. These tuffisites have just subtle δD depletions (-4–$5‰$; pairs 1 and 3) despite substantial H_2O drops (up to $\sim$ 0.9 wt.%) to large enrichments (up to $> -10‰$; pairs 6, 7, 9) relative to host obsidians. These D-enriched patterns are incompatible with both closed- and open-system degassing, which would cause moderate to extreme drops in δD, respectively, with falling bulk-H_2O content (Supplementary Information). Instead, these tuffisites must have equilibrated with a D-rich fluid, which would have dampened D/H fractionation during pyroclastic degassing within the veins (Dobson et al., 1989; Rust et al., 2004). Such a buffer gas could have come from deeper, less-degassed (and therefore more D-rich) magma, or from domains of hydrous magma adjacent to the veins. Thus, buffered degassing signatures imply that pyroclastic veins are at times chemically and physically "open" to their surroundings (Fig. 7b), and therefore capable of transmitting of far-travelled gas (Molina et al., 2004; Johnson et al., 2008; Berlo et al., 2013; Schipper et al., 2013) that could impart relatively juvenile H-isotopic signatures on pyroclasts and host magma degassing at shallow levels.

In summary, two distinct degassing modes are recorded at the cm-scale in tuffisite bombs—closed and open-buffered modes. These two mechanisms are entirely consistent with the batched degassing path used to explain the broad δD–H_2O pattern produced by Chaitén's explosive and effusive sequence (Fig. 6c). In particular the different isotopic signatures around the veins (closed and buffered) manifest the sequence of repetitive closed-system steps and intervening pulses of gas release that underpin the batched-degassing path. Whether or not the closed and open-buffered degassing signatures reflect temporal variations in the size, position, and geometry of veins remains an unanswered question. However, it seems possible that tuffisite veins may "cycle"

through various degassing modes as they are forced to either grow into larger networks, where they may penetrate into deeper magma, or remain isolated due to their limited extents or because they have welded shut (Yoshimura and Nakamura, 2010). In the dynamic environment of an explosively erupting silicic conduit, the conditions are indeed ripe for both opening and closing pyroclastic veins: vein networks can open and grow in response to shear deformation (Gonnermann and Manga, 2003; Cabrera et al., 2011; Okumura et al., 2013), explosive shockwave propagation (Alidibirov and Dingwell, 1996), or fluid pressurization and hydrofacturing (Heiken et al., 1988), or close due to pyroclast clogging and sintering of grains in the presence of abundant hot gas and overpressure (Westrich and Eichelberger, 1994; Tuffen et al., 2003; Cordonnier et al., 2012; Vasseur et al., 2013). Future work should examine rates and mechanisms of fluid and pyroclast transport through tuffisite veins, in addition to why these materials may stall, accumulate and therefore, create overpressure that is then explosively released in many hundreds of violent blasts during effusive rhyolite eruptions (Supplementary Video).

6. Concluding remarks

Although silicic lavas have been known to explosively vent at their collapsing flow fronts (Fink and Kieffer, 1993), or from late stage vesiculation at their surfaces (Fink et al., 1992), explosive processes have never been recognized to play a key role in degassing and thus making lava. We have demonstrated that a single batched degassing mechanism explains the chemical evolution of rhyolite magma across the explosive-to-effusive transition. Batched degassing is made possible by the physical behaviour of tuffisite veins, which through their transiently closed and open physical states, allow for local vapour storage but also very rapid separation of exsolved gas from magma, often with explosive consequences. A singular degassing mechanism that links explosive and effusive volcanism is also consistent with the behaviour of effusive rhyolite eruptions (Castro et al., 2012; Schipper et al., 2013), which are now known to be accompanied by pyroclastic activity and therefore perhaps not the hallmarks of quiet, non-explosive, open-system degassing (Eichelberger et al., 1986; Villemant and Boudon, 1998; Westrich and Eichelberger, 1994). Hazards assessment of future effusive silicic eruptions will improve with new eruption models that incorporate rates of melt embrittlement (Okumura et al., 2013), pyroclast and tuffisite degassing (Castro et al., 2012; Berlo et al., 2013), and welding (Tuffen et al., 2003; Vasseur et al., 2013) in silicic conduits.

7. Author contributions

J.M.C. conceived of the study, organized field campaigns, prepared samples for isotopic measurements, modelled isotopic data, and wrote the manuscript. I.N.B. performed isotopic measurements, interpreted data, and edited the manuscript. H.T., and C.I.S. interpreted data, drafted figures, and edited the manuscript.

Acknowledgements

The authors thank John Pallister and the U.S.G.S. Volcano Hazards Program, Catherine Amie Besch and Nicolas La Penna for field support. Jim Palandri provided valuable isotopic analyses. J.M.C. was supported by the Geocycles Research Centre. H.T. was supported by a Royal Society University Research Fellowship. This work was supported by the VAMOS Research Center at the University of Mainz. H. Gonnermann is thanked for his insightful comments on an earlier version of this manuscript. Caroline Martel and two anonymous reviewers provided useful comments. C.I.S. was supported by ERC grant 202844 under the EU.

Appendix A. Supplementary material

Supplementary material related to this article can be found online at http://dx.doi.org/10.1016/j.epsl.2014.08.012.

References

Adams, N.K., Houghton, B.F., Fagents, S.A., 2006. The transition from explosive to effusive eruption regime: the example of the 1912 Novarupta eruption, Alaska. Geol. Soc. Am. Bull. 118, 620–634.
Alfano, F., Bonadonna, C., Volentik, A.C.M., Conner, C.B., Watt, S.F.L., Pyle, D.M., Conner, L.J., 2011. Tephra stratigraphy and eruptive volume of the May, 2008, Chaitén eruption, Chile. Bull. Volcanol. 73, 613–630.
Alidibirov, M., Dingwell, D.B., 1996. Magma fragmentation by rapid decompression. Nature 380, 146–148.
Anderson, S.W., Fink, J.H., 1989. Hydrogen-isotope evidence for extrusion mechanisms of the Mount St. Helens lava dome. Nature 341, 521–523.
Berlo, K., Tuffen, H., Smith, V.C., Castro, J.M., Pyle, D.M., Mather, T.A., Geraki, K., 2013. Element variations in rhyolitic magma resulting from gas transport. Geochim. Cosmochim. Acta 121, 436–451.
Bindeman, I.N., Kamenetsky, V., Palandri, J., Vennemann, T., 2012. Hydrogen and oxygen isotope behavior during variable degrees of upper mantle melting: example from the basaltic glasses from Macquarie Island. Chem. Geol. 310–311, 126–136.
Cabrera, A., Weinberg, R.F., Wright, H., Zlotnik, S., Cas, R.A.F., 2011. Melt fracturing and healing: a mechanism for degassing and origin of silicic obsidian. Geology 39, 67–70.
Cashman, K.V., 2004. Volatile controls on magma ascent and eruption. Geophys. Monogr. 150 (19), 109–124.
Castro, J.M., Dingwell, D.B., 2009. Rapid ascent of rhyolite magma at Chaitén volcano. Nature 461, 780–783.
Castro, J.M., Mercer, C., 2004. Microlite textures and volatile contents of obsidian from the Inyo volcanic chain, California. Geophys. Res. Lett. 31, L18605. http://dx.doi.org/10.1029/2004GL020489.
Castro, J.M., Cordonnier, B., Tuffen, H., Tobin, M.J., Puskar, L., Martin, M.C., Bechtel, H.A., 2012. The role of melt-fracture degassing in defusing explosive rhyolite eruptions at volcán Chaitén. Earth Planet. Sci. Lett. 333–334, 63–69.
Castro, J.M., Schipper, C.I., Mueller, S.P., Militzer, A.S., Amigo, A., Parejas, C.S., Jacob, D., 2013. Storage and eruptions of near-liquidus rhyolite magma at Cordón Caulle, Chile. Bull. Volcanol. 75, 702–719.
Cordonnier, B., Caricchi, L., Pistone, M., Castro, J., Hess, K.-U., Gottschaller, S., Manga, M., Dingwell, D.B., Burlini, L., 2012. The viscous-brittle transition of crystal-bearing silicic melt: direct observation of magma rupture and healing. Geology 40, 611–614.
Dingwell, D.B., 1996. Volcanic dilemma: flow or blow? Science 273, 1054–1055.
Dobson, P.F., Epstein, S., Stolper, E.M., 1989. Hydrogen isotope fractionation between coexisting vapor and silicate glasses and melts at low pressure. Geochim. Cosmochim. Acta 53, 2723–2730.
Eichelberger, J.C., Westrich, H.R., 1981. Magmatic volatiles in explosive rhyolitic eruptions. Geophys. Res. Lett. 8, 757–760.
Eichelberger, J.C., Carrigan, C.R., Westrich, H.R., Price, R.H., 1986. Non-explosive silicic volcanism. Nature 323, 598–602.
Fink, J.H., Kieffer, S.W., 1993. Estimate of pyroclastic flow velocities resulting from explosive decompression of lava domes. Nature 363, 612–615.
Fink, J.H., Anderson, S.W., Manley, C.R., 1992. Textural constraints on effusive silicic volcanism: beyond the permeable foam model. J. Geophys. Res. 97, 9073–9083.
Gonnermann, H., Manga, M., 2003. Explosive volcanism may not be an inevitable consequence of magma fragmentation. Nature 426, 432–435.
Heiken, G., Wohletz, K., Eichelberger, J., 1988. Fracture fillings and intrusive pyroclasts, Inyo Domes, California. J. Geophys. Res. 93, 4335–4350.
Hildreth, W., Fierstein, J., 2000. Katmai volcanic cluster and the great eruption of 1912. Geol. Soc. Am. Bull. 112, 1594–1620.
Jaupart, C., Allègre, C.J., 1991. Gas content, eruption rate and instabilities of eruption regimes in silicic volcanoes. Earth Planet. Sci. Lett. 102, 413–429.
Johnson, J.B., Lees, J.M., Gerst, A., Sahagian, D., Varley, N., 2008. Long-period earthquakes and co-eruptive dome inflation seen with particle image velocimetry. Nature 456, 377–381.
Lara, L.E., 2009. The 2008 eruption of the Chaitén volcano, Chile: a preliminary report. Andean Geol. 36, 125–129.
Major, J.J., Lara, L.E., 2013. Overview of Chaitén Volcano, Chile, and its 2008–2009 eruption. Andean Geol. 40, 196–215.
Melson, W.G., Saenz, R., 1973. Volume, energy and cyclicity of eruptions of Arenal volcano, Costa Rica. Bull. Volcanol. 37, 416–437.
Molina, I., Kumagai, H., Yepes, H., 2004. Resonances of a volcanic triggered by repetitive injections of an ash-laden gas. Geophys. Res. Lett. 31, L03603.
Newman, S., Lowenstern, J.B., 2002. VolatileCalc: a silicate melt-H_2O–CO_2 solution model written in visual Basic for Excel. Comput. Geosci. 28, 597–604.

Newman, S., Epstein, S., Stolper, E., 1988. Water, carbon dioxide, and hydrogen isotopes in glasses from the ca. 1340 A.D. eruption of the Mono Craters, California: constraints on degassing phenomena and initial volatile content. J. Volcanol. Geotherm. Res. 35, 75–96.

Nguyen, C.T., Gonnermann, H.M., Houghton, B.F., 2014. Explosive to effusive transition during the largest volcanic eruption of the 20th century (Novarupta 1912, Alaska). Geology. http://dx.doi.org/10.1130/G35593.1.

Nolan, G.S., Bindeman, I.N., 2013. Experimental investigation of rates and mechanisms of isotope exchange (O, H) between volcanic ash and isotopically-labeled water. Geochim. Cosmochim. Acta 111, 5–27.

Okumura, S., Nakamura, M., Takeuchi, S., Tsuchiyama, A., Nakano, T., Uesugi, K., 2009. Magma deformation may induce non-explosive volcanism via degassing through bubble networks. Earth Planet. Sci. Lett. 281, 267–274.

Okumura, S., Nakamura, M., Nakano, T., Uesugi, K., Tsuchiyama, A., 2010. Shear deformation experiments on vesicular rhyolite: implications for brittle fracturing, degassing, and compaction of magmas in volcanic conduits. J. Geophys. Res. 115, B06201.

Okumura, S., Nakamura, M., Uesugi, K., Nakano, T., Fujioka, T., 2013. Coupled effect of magma degassing and rheology on silicic volcanism. Earth Planet. Sci. Lett. 362, 163–170.

Papale, P., 1999. Strain-induced magma fragmentation in explosive eruptions. Nature 397, 425–428.

Rust, A.D., Cashman, K.V., 2007. Multiple origins of obsidian pyroclasts an implications for changes in the dynamics of the 1300 B.P. eruption of Newberry Volcano, USA. Bull. Volcanol. 69, 825–845.

Rust, A.C., Cashman, K.V., Wallace, P., 2004. Magma degassing buffered by vapour flow through brecciated conduit margins. Geology 32, 349–352.

Schipper, C.I., Castro, J.M., Tuffen, H., James, M.R., How, P., 2013. Shallow vent architecture during hybrid explosive–effusive activity at Cordón Caulle (Chile, 2011–12): evidence from direct observations and pyroclast textures. J. Volcanol. Geotherm. Res. 262, 25–37.

Sparks, R.S.J., 1978. The dynamics of bubble formation and growth in magmas: a review and analysis. J. Volcanol. Geotherm. Res. 3, 1–37.

Stasiuk, M.V., Barclay, J., Carroll, M.R., Jaupart, C., Ratté, J.C., Sparks, R.S.J., Tait, S.R., 1996. Degassing during magma ascent in the Mule Creek vent (USA). Bull. Volcanol. 58, 117–130.

Taylor, B.E., 1991. Degassing of Obsidian Dome rhyolite, Inyo volcanic chain, California. In: Taylor Jr., H.P., O'Neil, J.R., Kaplan, J.R. (Eds.), Stable Isotope Geochemistry: A Tribute to Samuel Epstein. In: Geochemical Society Special Publication, vol. 3. The Geochemical Society, San Antonio, TX, pp. 339–353.

Taylor, B.E., Eichelberger, J.C., Westrich, H.R., 1983. Hydrogen isotopic evidence of rhyolitic magma degassing during shallow intrusion and eruption. Nature 306, 541–545.

Tuffen, H., Dingwell, D.B., 2005. Fault textures in volcanic conduits: evidence for seismic trigger mechanisms during silicic eruptions. Bull. Volcanol. 67, 370–387.

Tuffen, H., Dingwell, D.B., Pinkerton, H., 2003. Repeated fracture and healing of silicic magma generate flow banding and earthquakes? Geology 31, 1089–1092.

Tuffen, H., James, M.R., Castro, J.M., Schipper, C.I., 2013. Exceptional mobility of an advancing rhyolitic obsidian flow at Cordón Caulle volcano in Chile. Nat. Commun. 4, 2709.

Vasseur, J., Wadsworth, F.B., Lavallée, Y., Hess, K.-U., Dingwell, D.B., 2013. Volcanic sintering: timescales of viscous densification and strength recovery. Geophys. Res. Lett. 40, 1–7.

Villemant, B., Boudon, G., 1998. Transition from dome-forming to plinian eruptive styles controlled by H_2O and Cl degassing. Nature 392, 65–69.

Watkins, J.M., Manga, M., DePaolo, D.J., 2012. Bubble geobarometry: a record of pressure changes, degassing and regassing at Mono Craters, California. Geology 40, 699–702.

Westrich, H.R., Eichelberger, J.C., 1994. Gas transport and bubble collapse in rhyolitic magma: an experimental approach. Bull. Volcanol. 56, 447–458.

Wilson, L., 1976. Explosive volcanic eruptions—III. Plinian Eruption Columns. Geophys. J. R. Astron. Soc. 45, 543–556.

Woods, A.W., Koyaguchi, T., 1994. Transitions between explosive and effusive eruptions of silicic magmas. Nature 370, 641–644.

Yoshimura, S., Nakamura, M., 2010. Fracture healing in a magma: an experimental approach and implications for volcanic seismicity and degassing. J. Geophys. Res. 115, B09209.